Search for Darkonium in e^+e^- Collisions

J. P. Lees,[1] V. Poireau,[1] V. Tisserand,[1] E. Grauges,[2] A. Palano,[3] G. Eigen,[4] D. N. Brown,[5] Yu. G. Kolomensky,[5] M. Fritsch,[6] H. Koch,[6] T. Schroeder,[6] R. Cheaib,[7b] C. Hearty,[7a,7b] T. S. Mattison,[7b] J. A. McKenna,[7b] R. Y. So,[7b] V. E. Blinov,[8a,8b,8c] A. R. Buzykaev,[8a] V. P. Druzhinin,[8a,8b] V. B. Golubev,[8a,8b] E. A. Kozyrev,[8a,8b] E. A. Kravchenko,[8a,8b] A. P. Onuchin,[8a,8b,8c,*] S. I. Serednyakov,[8a,8b] Yu. I. Skovpen,[8a,8b] E. P. Solodov,[8a,8b] K. Yu. Todyshev,[8a,8b] A. J. Lankford,[9] B. Dey,[10] J. W. Gary,[10] O. Long,[10] A. M. Eisner,[11] W. S. Lockman,[11] W. Panduro Vazquez,[11] D. S. Chao,[12] C. H. Cheng,[12] B. Echenard,[12] K. T. Flood,[12] D. G. Hitlin,[12] J. Kim,[12] Y. Li,[12] D. X. Lin,[12] T. S. Miyashita,[12] P. Ongmongkolkul,[12] J. Oyang,[12] F. C. Porter,[12] M. Röhrken,[12] Z. Huard,[13] B. T. Meadows,[13] B. G. Pushpawela,[13] M. D. Sokoloff,[13] L. Sun,[13,†] J. G. Smith,[14] S. R. Wagner,[14] D. Bernard,[15] M. Verderi,[15] D. Bettoni,[16a] C. Bozzi,[16a] R. Calabrese,[16a,16b] G. Cibinetto,[16a,16b] E. Fioravanti,[16a,16b] I. Garzia,[16a,16b] E. Luppi,[16a,16b] V. Santoro,[16a] A. Calcaterra,[17] R. de Sangro,[17] G. Finocchiaro,[17] S. Martellotti,[17] P. Patteri,[17] I. M. Peruzzi,[17] M. Piccolo,[17] M. Rotondo,[17] A. Zallo,[17] S. Passaggio,[18] C. Patrignani,[18,‡] B. J. Shuve,[19] H. M. Lacker,[20] B. Bhuyan,[21] U. Mallik,[22] C. Chen,[23] J. Cochran,[23] S. Prell,[23] A. V. Gritsan,[24] N. Arnaud,[25] M. Davier,[25] F. Le Diberder,[25] A. M. Lutz,[25] G. Wormser,[25] D. J. Lange,[26] D. M. Wright,[26] J. P. Coleman,[27] E. Gabathuler,[27,*] D. E. Hutchcroft,[27] D. J. Payne,[27] C. Touramanis,[27] A. J. Bevan,[28] F. Di Lodovico,[28,§] R. Sacco,[28] G. Cowan,[29] Sw. Banerjee,[30] D. N. Brown,[30] C. L. Davis,[30] A. G. Denig,[31] W. Gradl,[31] K. Griessinger,[31] A. Hafner,[31] K. R. Schubert,[31] R. J. Barlow,[32,∥] G. D. Lafferty,[32] R. Cenci,[33] A. Jawahery,[33] D. A. Roberts,[33] R. Cowan,[34] S. H. Robertson,[35a,35b] R. M. Seddon,[35b] N. Neri,[36a] F. Palombo,[36a,36b] L. Cremaldi,[37] R. Godang,[37,¶] D. J. Summers,[37,*] P. Taras,[38] G. De Nardo,[39] C. Sciacca,[39] G. Raven,[40] C. P. Jessop,[41] J. M. LoSecco,[41] K. Honscheid,[42] R. Kass,[42] A. Gaz,[43a] M. Margoni,[43a,43b] M. Posocco,[43a] G. Simi,[43a,43b] F. Simonetto,[43a,43b] R. Stroili,[43a,43b] S. Akar,[44] E. Ben-Haim,[44] M. Bomben,[44] G. R. Bonneaud,[44] G. Calderini,[44] J. Chauveau,[44] G. Marchiori,[44] J. Ocariz,[44] M. Biasini,[45a,45b] E. Manoni,[45a] A. Rossi,[45a] G. Batignani,[46a,46b] S. Bettarini,[46a,46b] M. Carpinelli,[46a,46b,**] G. Casarosa,[46a,46b] M. Chrzaszcz,[46a] F. Forti,[46a,46b] M. A. Giorgi,[46a,46b] A. Lusiani,[46a,46c] B. Oberhof,[46a,46b] E. Paoloni,[46a,46b] M. Rama,[46a] G. Rizzo,[46a,46b] J. J. Walsh,[46a] L. Zani,[46a,46b] A. J. S. Smith,[47] F. Anulli,[48a] R. Faccini,[48a,48b] F. Ferrarotto,[48a] F. Ferroni,[48a,††] A. Pilloni,[48a,48b] G. Piredda,[48a,*] C. Bünger,[49] S. Dittrich,[49] O. Grünberg,[49] M. Heß,[49] T. Leddig,[49] C. Voß,[49] R. Waldi,[49] T. Adye,[50] F. F. Wilson,[50] S. Emery,[51] G. Vasseur,[51] D. Aston,[52] C. Cartaro,[52] M. R. Convery,[52] J. Dorfan,[52] W. Dunwoodie,[52] M. Ebert,[52] R. C. Field,[52] B. G. Fulsom,[52] M. T. Graham,[52] C. Hast,[52] W. R. Innes,[52,*] P. Kim,[52] D. W. G. S. Leith,[52,*] S. Luitz,[52] D. B. MacFarlane,[52] D. R. Muller,[52] H. Neal,[52] B. N. Ratcliff,[52] A. Roodman,[52] M. K. Sullivan,[52] J. Va'vra,[52] W. J. Wisniewski,[52] M. V. Purohit,[53] J. R. Wilson,[53] A. Randle-Conde,[54] S. J. Sekula,[54] H. Ahmed,[55] M. Bellis,[56] P. R. Burchat,[56] E. M. T. Puccio,[56] M. S. Alam,[57] J. A. Ernst,[57] R. Gorodeisky,[58] N. Guttman,[58] D. R. Peimer,[58] A. Soffer,[58] S. M. Spanier,[59] J. L. Ritchie,[60] R. F. Schwitters,[60] J. M. Izen,[61] X. C. Lou,[61] F. Bianchi,[62a,62b] F. De Mori,[62a,62b] A. Filippi,[62a] D. Gamba,[62a,62b] L. Lanceri,[63] L. Vitale,[63] F. Martinez-Vidal,[64] A. Oyanguren,[64] J. Albert,[65b] A. Beaulieu,[65b] F. U. Bernlochner,[65b] G. J. King,[65b] R. Kowalewski,[65b] T. Lueck,[65b] I. M. Nugent,[65b] J. M. Roney,[65b] R. J. Sobie,[65a,65b] N. Tasneem,[65b] T. J. Gershon,[66] P. F. Harrison,[66] T. E. Latham,[66] R. Prepost,[67] and S. L. Wu[67]

(*BaBar* Collaboration)

[1]*Laboratoire d'Annecy-le-Vieux de Physique des Particules (LAPP), Université de Savoie, CNRS/IN2P3, F-74941 Annecy-Le-Vieux, France*
[2]*Universitat de Barcelona, Facultat de Fisica, Departament ECM, E-08028 Barcelona, Spain*
[3]*INFN Sezione di Bari, I-70126 Bari, Italy*
[4]*University of Bergen, Institute of Physics, N-5007 Bergen, Norway*
[5]*Lawrence Berkeley National Laboratory and University of California, Berkeley, California 94720, USA*
[6]*Ruhr Universität Bochum, Institut für Experimentalphysik 1, D-44780 Bochum, Germany*
[7a]*Institute of Particle Physics, Vancouver, British Columbia V6T 1Z1, Canada*
[7b]*University of British Columbia, Vancouver, British Columbia V6T 1Z1, Canada*
[8a]*Budker Institute of Nuclear Physics SB RAS, Novosibirsk 630090, Russia*
[8b]*Novosibirsk State University, Novosibirsk 630090, Russia*
[8c]*Novosibirsk State Technical University, Novosibirsk 630092, Russia*
[9]*University of California at Irvine, Irvine, California 92697, USA*
[10]*University of California at Riverside, Riverside, California 92521, USA*
[11]*University of California at Santa Cruz, Institute for Particle Physics, Santa Cruz, California 95064, USA*

[12]California Institute of Technology, Pasadena, California 91125, USA
[13]University of Cincinnati, Cincinnati, Ohio 45221, USA
[14]University of Colorado, Boulder, Colorado 80309, USA
[15]Laboratoire Leprince-Ringuet, Ecole Polytechnique, CNRS/IN2P3, F-91128 Palaiseau, France
[16a]INFN Sezione di Ferrara, I-44122 Ferrara, Italy
[16b]Dipartimento di Fisica e Scienze della Terra, Università di Ferrara, I-44122 Ferrara, Italy
[17]INFN Laboratori Nazionali di Frascati, I-00044 Frascati, Italy
[18]INFN Sezione di Genova, I-16146 Genova, Italy
[19]Harvey Mudd College, Claremont, California 91711, USA
[20]Humboldt-Universität zu Berlin, Institut für Physik, D-12489 Berlin, Germany
[21]Indian Institute of Technology Guwahati, Guwahati, Assam 781 039, India
[22]University of Iowa, Iowa City, Iowa 52242, USA
[23]Iowa State University, Ames, Iowa 50011, USA
[24]Johns Hopkins University, Baltimore, Maryland 21218, USA
[25]Université Paris-Saclay, CNRS/IN2P3, IJCLab, F-91405 Orsay, France
[26]Lawrence Livermore National Laboratory, Livermore, California 94550, USA
[27]University of Liverpool, Liverpool L69 7ZE, United Kingdom
[28]Queen Mary, University of London, London, E1 4NS, United Kingdom
[29]University of London, Royal Holloway and Bedford New College, Egham, Surrey TW20 0EX, United Kingdom
[30]University of Louisville, Louisville, Kentucky 40292, USA
[31]Johannes Gutenberg-Universität Mainz, Institut für Kernphysik, D-55099 Mainz, Germany
[32]University of Manchester, Manchester M13 9PL, United Kingdom
[33]University of Maryland, College Park, Maryland 20742, USA
[34]Massachusetts Institute of Technology, Laboratory for Nuclear Science, Cambridge, Massachusetts 02139, USA
[35a]Institute of Particle Physics, Montréal, Québec, Canada H3A 2T8
[35b]McGill University, Montréal, Québec, Canada H3A 2T8
[36a]INFN Sezione di Milano, I-20133 Milano, Italy
[36b]Dipartimento di Fisica, Università di Milano, I-20133 Milano, Italy
[37]University of Mississippi, University, Mississippi 38677, USA
[38]Université de Montréal, Physique des Particules, Montréal, Québec H3C 3J7, Canada
[39]INFN Sezione di Napoli and Dipartimento di Scienze Fisiche, Università di Napoli Federico II, I-80126 Napoli, Italy
[40]NIKHEF, National Institute for Nuclear Physics and High Energy Physics, NL-1009 DB Amsterdam, Netherlands
[41]University of Notre Dame, Notre Dame, Indiana 46556, USA
[42]The Ohio State University, Columbus, Ohio 43210, USA
[43a]INFN Sezione di Padova, I-35131 Padova, Italy
[43b]Dipartimento di Fisica, Università di Padova, I-35131 Padova, Italy
[44]Laboratoire de Physique Nucléaire et de Hautes Energies, Sorbonne Université, Paris Diderot Sorbonne Paris Cité, CNRS/IN2P3, F-75252 Paris, France
[45a]INFN Sezione di Perugia, I-06123 Perugia, Italy
[45b]Dipartimento di Fisica, Università di Perugia, I-06123 Perugia, Italy
[46a]INFN Sezione di Pisa, I-56127 Pisa, Italy
[46b]Dipartimento di Fisica, Università di Pisa, I-56127 Pisa, Italy
[46c]Scuola Normale Superiore di Pisa, I-56127 Pisa, Italy
[47]Princeton University, Princeton, New Jersey 08544, USA
[48a]INFN Sezione di Roma, I-00185 Roma, Italy
[48b]Dipartimento di Fisica, Università di Roma La Sapienza, I-00185 Roma, Italy
[49]Universität Rostock, D-18051 Rostock, Germany
[50]Rutherford Appleton Laboratory, Chilton, Didcot, Oxon OX11 0QX, United Kingdom
[51]IRFU, CEA, Université Paris-Saclay, F-91191 Gif-sur-Yvette, France
[52]SLAC National Accelerator Laboratory, Stanford, California 94309 USA
[53]University of South Carolina, Columbia, South Carolina 29208, USA
[54]Southern Methodist University, Dallas, Texas 75275, USA
[55]St. Francis Xavier University, Antigonish, Nova Scotia B2G 2W5, Canada
[56]Stanford University, Stanford, California 94305, USA
[57]State University of New York, Albany, New York 12222, USA
[58]Tel Aviv University, School of Physics and Astronomy, Tel Aviv 69978, Israel
[59]University of Tennessee, Knoxville, Tennessee 37996, USA
[60]University of Texas at Austin, Austin, Texas 78712, USA
[61]University of Texas at Dallas, Richardson, Texas 75083, USA
[62a]INFN Sezione di Torino, I-10125 Torino, Italy

[62b]Dipartimento di Fisica, Università di Torino, I-10125 Torino, Italy
[63]INFN Sezione di Trieste and Dipartimento di Fisica, Università di Trieste, I-34127 Trieste, Italy
[64]IFIC, Universitat de Valencia-CSIC, E-46071 Valencia, Spain
[65a]Institute of Particle Physics, Victoria, British Columbia V8W 3P6, Canada
[65b]University of Victoria, Victoria, British Columbia V8W 3P6, Canada
[66]Department of Physics, University of Warwick, Coventry CV4 7AL, United Kingdom
[67]University of Wisconsin, Madison, Wisconsin 53706, USA

(Received 20 June 2021; revised 17 September 2021; accepted 13 December 2021; published 11 January 2022)

Collider searches for dark sectors, new particles interacting only feebly with ordinary matter, have largely focused on identifying signatures of new mediators, leaving much of dark sector structures unexplored. In particular, the existence of dark matter bound states (darkonia) remains to be investigated. This possibility could arise in a simple model in which a dark photon (A') is light enough to generate an attractive force between dark fermions. We report herein a search for a $J^{PC} = 1^{--}$ darkonium state, the Υ_D, produced in the reaction $e^+e^- \to \gamma\Upsilon_D$, $\Upsilon_D \to A'A'A'$, where the dark photons subsequently decay into pairs of leptons or pions, using 514 fb^{-1} of data collected with the *BABAR* detector. No significant signal is observed, and we set bounds on the $\gamma - A'$ kinetic mixing as a function of the dark sector coupling constant for $0.001 < m_{A'} < 3.16$ GeV and $0.05 < m_{\Upsilon_D} < 9.5$ GeV.

DOI: 10.1103/PhysRevLett.128.021802

The possibility of dark sectors, new quantum fields neutral under all standard model (SM) forces, has emerged as an intriguing framework to explain the presence of dark matter in the Universe [1,2]. While these particles do not couple directly to ordinary matter, indirect interactions through low-dimensional operators called "portals" are possible [3]. The physics of these dark sectors could involve an arbitrary number of fields and interactions, including the possibility of self-interacting dark matter. This scenario can be realized in a minimal dark sector model containing a single Dirac fermion (χ) charged under a new U(1) gauge group with a coupling constant g_D [4]. The corresponding force carrier is conventionally referred to as a dark photon (A'), and couples to the SM photon via kinetic mixing with strength ε [5,6]. A low-mass dark photon would give rise to an attractive force between the χ and $\bar{\chi}$ particles, resulting in the formation of bound states (darkonia) when $1.68 m_{A'} < \alpha_D m_\chi$ for $\alpha_D = g_D^2/4\pi$ [4,7].

The two lowest energy bound states in this model are denoted η_D ($J^{PC} = 0^{-+}$) and Υ_D ($J^{PC} = 1^{--}$), in analogy with similar SM states. The quantum numbers predict the following production and decay mechanisms at e^+e^- colliders: $e^+e^- \to \eta_D + A'$, $\eta_D \to A'A'$ and initial-state radiation (ISR) process $e^+e^- \to \Upsilon_D + \gamma_{\mathrm{ISR}}$, $\Upsilon_D \to A'A'A'$. In the regime $m_{A'} < 2m_\chi$, the dark photon decays visibly into a pair of SM fermions with a decay width proportional to the product $m_{A'}\varepsilon^2$. Depending on the value of these parameters, the decays can be prompt or significantly displaced from the e^+e^- interaction point. Current constraints on visible A' decays [8–18] exclude values of $\varepsilon \gtrsim 10^{-3}$ over a wide range of masses from the dielectron threshold up to tens of GeV [19].

We report herein a search for darkonium in the ISR process $e^+e^- \to \gamma_{\mathrm{ISR}}\Upsilon_D$, $\Upsilon_D \to A'A'A'$, where the dark photons subsequently decay into pairs of electrons, muons, or pions. The cross section is determined for prompt A' decays in the region 0.001 GeV $< m_{A'} <$ 3.16 GeV and 0.05 GeV $< m_{\Upsilon_D} <$ 9.5 GeV. For $m_{A'} \geq 0.2$ GeV, the flight distance in the detector is smaller than 0.01 mm, effectively indistinguishable from prompt decays. For $m_{A'} < 0.2$ GeV, the dark photon decay length becomes significant for values of ε we expect to probe, and we additionally report cross sections for lifetimes $\tau_{A'}$ corresponding to $c\tau_{A'}$ values of 0.1, 1, and 10 mm. This search is based on 514 fb^{-1} of data collected with the *BABAR* detector at the SLAC PEP-II e^+e^- collider at the $\Upsilon(4S)$, $\Upsilon(3S)$, and $\Upsilon(2S)$ resonances and their vicinities [20]. The *BABAR* detector is described in detail elsewhere [21,22]. To avoid experimental bias, the data are not examined until the selection procedure is finalized. The analysis is developed using simulated signal events and a small fraction of real data for background studies.

Signal events are generated using MADGRAPH5 [23] with prompt dark photon decays for 119 different A' and Υ_D mass hypotheses. For $m_{A'} < 0.2$ GeV, we also simulate samples with non-zero dark photon lifetimes corresponding to proper decay lengths 0.1, 1, and 10 mm. The detector acceptance and reconstruction efficiencies are estimated with a simulation based on GEANT4 [24]. Since the background is too complex to be accurately simulated, we use 5% of the data together with the simulated signal samples to optimize the selection criteria, assuming that any signal component has a negligible impact on this procedure. This data set, referred to as the optimization sample, is discarded from the final results.

The event selection for prompt A' decays proceeds by selecting events containing exactly six charged tracks, and reconstructing dark photon candidates as pairs of oppositely charged tracks identified as electrons, muons, or pions by particle identification algorithms. We require the presence of at least one lepton pair of opposite charge with the same flavor to limit the large accidental background. We form Υ_D candidates by combining three dark photon candidates, and fit them, constraining all tracks to originate from a common point compatible with the beam interaction region. For each Υ_D candidate, we additionally form same-sign track combinations by swapping particles with identical flavor between reconstructed A' pairs, such as $(e^+e^+)(e^-e^-)(\mu^+\mu^-)$ or $(\pi^+\pi^+)(\pi^-\pi^-)(e^+e^-)$. For the fully mixed final state $(\mu^+\mu^-)(\pi^+\pi^-)(e^+e^-)$, we use the same-sign combination $(\mu^+\pi^+)(\mu^-\pi^-)(e^+e^-)$, since pions are more easily misidentified as muons than electrons. Because of the combinatoric nature of the background, the distributions of the mass difference for same-sign and opposite-sign pairs tend to be similar. By contrast, the differences between these distributions tend to be larger for signal events, effectively providing discrimination power.

The detection of the ISR photon accompanying Υ_D production is not explicitly required. Instead, we infer the kinematics of the particle recoiling against the Υ_D candidates, and we select the ISR photon candidate that is most compatible with the photon hypothesis as follows. If the recoil particle is determined to have been emitted inside the electromagnetic calorimeter acceptance, we search for the presence of a corresponding ISR photon candidate, which is defined as a neutral cluster having an energy within 10% of that of the recoiling particle, and an angle compatible with the direction of the recoiling particle to better than 0.1 rad.

To improve the signal purity, we train three multivariate classifiers consisting of logistic regressions stacked on top of random forest (RF) classifiers [25]. The following 13 variables are used as inputs to the RF: the χ^2 of the constrained fit to the Υ_D candidate; combined particle identification information of the six tracks; the maximum mass difference between any pair of A' candidates; the polar angle and the invariant mass of the particle recoiling against the reconstructed Υ_D candidate; a categorical feature indicating whether the recoiling particle is emitted inside the calorimeter acceptance and if a corresponding ISR photon candidate is found; the sum of neutral energy deposited in the electromagnetic calorimeter, excluding the ISR photon candidate; the average of the three dark photon helicity angles [26]; the average of the angles between pairs of dark photons in the Υ_D rest frame; the average of the dihedral angles between pairs of dark photons; the average of the three helicity angles of the tracks produced in the A' decays; the average of the dark photon decay lengths, defined as the distances between the primary interaction point and the A' decay vertices; and the maximum mass difference between same-sign pairs.

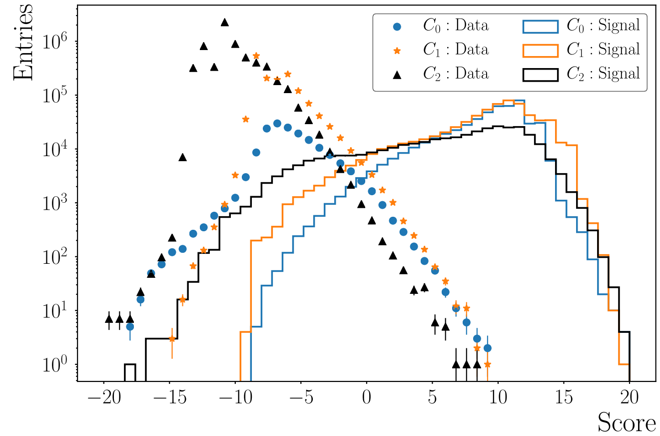

FIG. 1. The distribution of the classifier scores for each event category for the data (markers) and signal Monte Carlo (solid lines) samples. The MC simulations are arbitrarily normalized.

To improve the robustness of the predictions of the classifiers, we group the final states into three categories based on the number of pion pairs: zero (C_0), one (C_1), or two (C_2) pion pairs. A classifier is trained for each category with a sample of simulated events for different Υ_D and A' masses and a fraction of the optimization sample to describe the background. The classifier outputs are then transformed into classifier scores using a logit function [27], with higher scores indicating greater probabilities of being signal events. The distribution of the classifier scores for each category are shown in Fig. 1. The optimal selection criteria are determined by maximizing a figure of merit averaged over a wide range of Υ_D and A' masses. We adopt a conservative approach and treat observed events as signal candidates for the purposes of calculating the figure of merit. If multiple Υ_D candidates are selected in an event, a single one is chosen based on its final state according to the following sequence of hypotheses: $6e$, $4e2\mu$, $2e4\mu$, 6μ, $4e2\pi$, $2e2\mu2\pi$, $4\mu2\pi$, $2e4\pi$, $2\mu4\pi$. The sequence of hypotheses is ordered according to the purity of the final states to minimize misidentification between channels.

A total of 69 events pass all the selection criteria. The corresponding $(m_{\Upsilon_D}, m_{A'})$ distribution is shown in Fig. 2. The events near $m_{\Upsilon_D} \sim 0.1$ GeV and $m_{A'} \sim 0.05$ GeV arise from $e^+e^- \to \gamma\gamma\gamma$ events in which all three photons convert to e^+e^- pairs.

The signal is extracted by combining all event categories into a single sample, and scanning the $(m_{\Upsilon_D}, m_{A'})$ plane in steps of the signal resolution. The signal region for a given mass hypothesis is defined as the interval $[m_{\Upsilon_D} - 4\sigma_{m_{\Upsilon_D}}; m_{\Upsilon_D} + 4\sigma_{m_{\Upsilon_D}}]$ and $[m_{A'} - 4\sigma_{m_{A'}}; m_{A'} + 4\sigma_{m_{A'}}]$, where

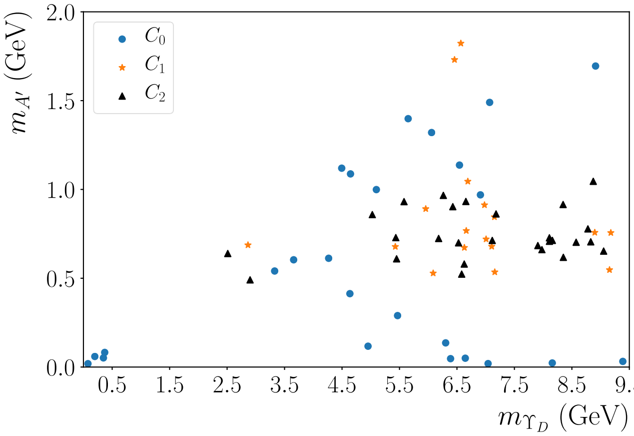

FIG. 2. The $(m_{\Upsilon_D}, m_{A'})$ distribution for events passing all selection criteria for prompt dark photon decays.

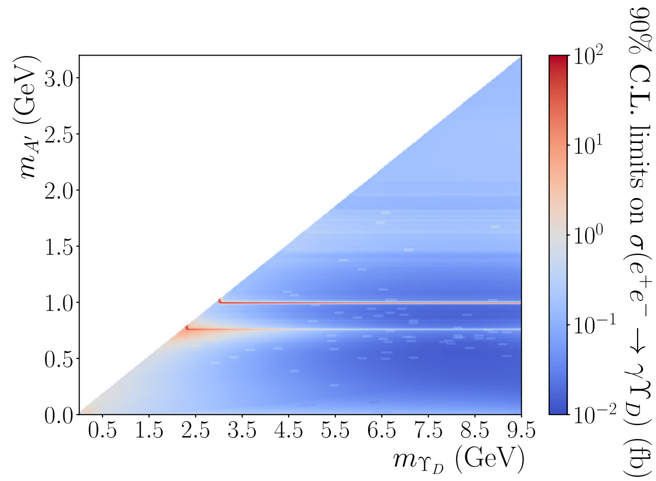

FIG. 3. The 90% C.L. upper limits on the $e^+e^- \to \gamma\Upsilon_D$ cross section for prompt dark photon decays.

$\sigma_{m_{\Upsilon_D}}$ ($\sigma_{m_{A'}}$) denotes the corresponding Υ_D (A') mass resolution. The resolutions are determined by fitting the different signal Monte Carlo (MC) samples with a crystal ball function [28] and interpolating the results throughout the full mass range. The Υ_D (A') mass resolution varies between 5–40 MeV (1–8 MeV); the detailed results are available in Supplemental Material [29]. The number of observed background events is estimated by averaging two neighboring regions along the m_{Υ_D} axis: $[m_{\Upsilon_D} - 8\sigma_{m_{\Upsilon_D}}; m_{\Upsilon_D} - 4\sigma_{m_{\Upsilon_D}}]$ and $[m_{\Upsilon_D} + 4\sigma_{m_{\Upsilon_D}}; m_{\Upsilon_D} + 8\sigma_{m_{\Upsilon_D}}]$. This choice is motivated by the potential background contribution due to hadronic resonances or photon conversions, which would be concentrated at similar values of dark photon masses. The signal significance is assessed from MC samples, using sideband data from the classifier score distribution to model the $(m_{\Upsilon_D}, m_{A'})$ distribution of the background. The most significant measurement contains two events in the signal window, corresponding to a p value of 30%, which is compatible with the null hypothesis.

In the absence of signal, we derive 90% confidence level (C.L.) upper limits on the $e^+e^- \to \gamma\Upsilon_D$ cross section using a profile likelihood method [30]. The probability of observing N events in a given signal region is described by the following model:

$$P(N|n+b) = \frac{e^{-n}n^N}{N!}\frac{e^{-b}b^B}{B!}\frac{1}{2\pi\sigma_Z\sigma_L}e^{[-(z-Z)^2/2\sigma_Z^2]}e^{[-(l-L)^2/2\sigma_L^2]},$$

where b (B) is the expected (estimated) number of background events, and $n = lz\sigma(e^+e^- \to \gamma\Upsilon_D)$ is the expected number of signal events given by the product of the integrated luminosity l, the $e^+e^- \to \gamma\Upsilon_D$ cross section, and the signal efficiency z. The measured luminosity, signal efficiency, and their uncertainties are denoted by L, Z, σ_L, and σ_Z, respectively. The signal efficiency includes the dark photon branching fractions, taken from Ref. [31]. The efficiency is determined for each simulated sample and interpolated to the full parameter space, ranging from 0.1% for $m_{\Upsilon_D} \sim 0.15$ GeV, $m_{A'} \sim 0.05$ GeV to 34% for $m_{\Upsilon_D} \sim 8.0$ GeV, $m_{A'} \sim 1.0$ GeV. The uncertainty in the signal efficiency arises mainly from particle identification algorithms, assessed with high-purity samples of leptons and pions. This source of uncertainty varies between 9% and 11%. The uncertainty associated with the efficiency extrapolation procedure ranges from 4% to 7%, depending on the m_{Υ_D} and $m_{A'}$. Other uncertainties include the tracking efficiency (1.2%) and the limited statistical precision of the simulated sample (1%–5%). The uncertainty in the dark photon branching fraction [31] ranges from parts per mille to 1%. The uncertainty in the luminosity is determined to be 0.6% [20]. The cross section at 90% C.L. upper limits are displayed in Fig. 3. The dark photon decays predominantly into $\pi^+\pi^-\pi^0$ (K^+K^-) near the ω (ϕ) resonance which are not considered

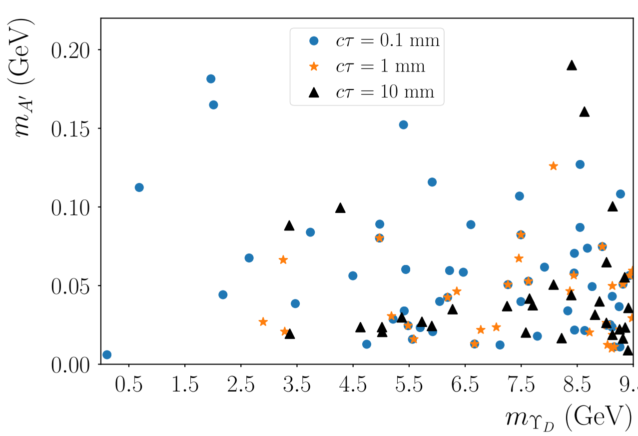

FIG. 4. The $(m_{\Upsilon_D}, m_{A'})$ mass distribution of event candidates passing all selection criteria for the datasets optimized for each dark photon lifetime.

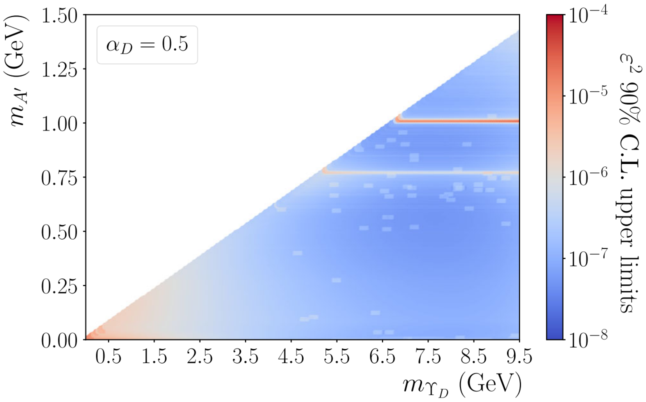

FIG. 5. The 90% C.L. upper limits on the kinetic mixing ε^2 as a function of the Υ_D mass m_{Υ_D} and dark photon mass $m_{A'}$, assuming $\alpha_D = 0.5$.

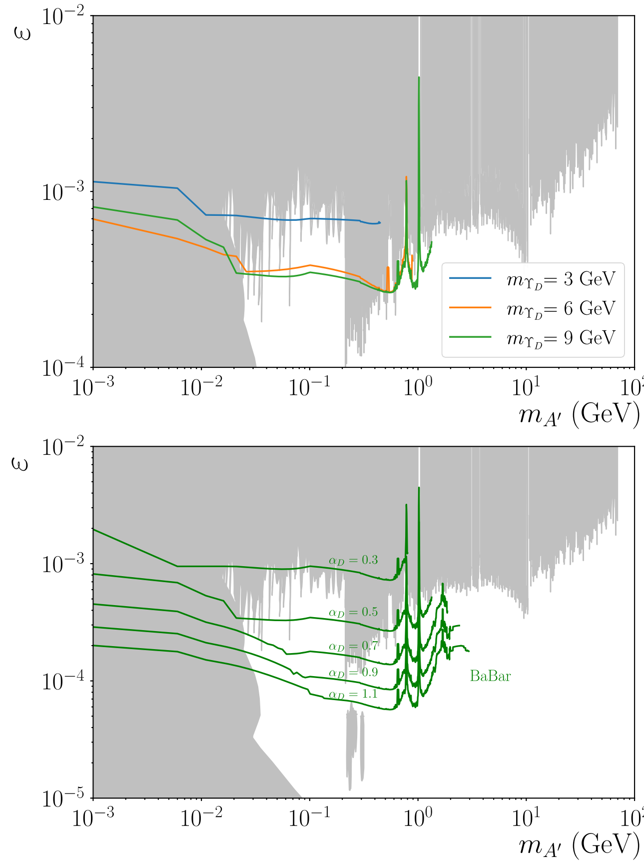

FIG. 6. The 90% C.L. upper limits on the kinetic mixing ε for (top) various Υ_D masses assuming $\alpha_D = 0.5$ and (bottom) various α_D values assuming $m_{\Upsilon_D} = 9$ GeV together with current constraints (gray area) [8–18].

in this analysis, resulting in much looser bounds around $m_{A'} \sim 0.8$ GeV ($m_{A'} \sim 1$ GeV).

We follow a similar procedure to determine the $e^+e^- \to \gamma\Upsilon_D$ cross section for each dark photon lifetime hypothesis. The measurement is performed for $m_{A'} < 0.2$ GeV. In this mass range, the A' decays almost exclusively to an e^+e^- pair. The event selection is analogous to that previously described, except that we constrain the momentum vector of the A' candidates to point back to the beam interaction region instead of requiring the tracks to originate from this location when performing the Υ_D kinematic fit. To further suppress photon conversions in the detector material, we add the following variables to the RF classifier, averaged over the three dark photon candidates: the χ^2 of a fit of the A' candidate; the angle between the secondary vertex flight direction and the A' momentum; and the ratio between the flight length and its uncertainty. We train a classifier for each $c\tau_{A'}$ value to improve the search sensitivity. A total of 56, 33, and 31 events are selected for the $c\tau_{A'} = 0.1$, 1, and 10 mm data sample, respectively. The resulting mass distributions are shown in Fig. 4. The signal extraction procedure described above is applied to each selected sample separately. No significant signal is observed for any A' lifetime hypothesis, and limits on the cross section for each value of $c\tau_{A'}$ are extracted. The classifier score distributions and the cross section at 90% C.L. upper limits are shown in Supplemental Material [29].

The 90% C.L. upper limits on the kinetic mixing parameter are extracted by an iterative procedure taking into account the effect of the potentially long dark photon lifetime. At each step, we estimate the dark photon lifetime given the current value of the kinetic mixing, compare the limit on the production cross section interpolated at that lifetime, update the kinetic mixing, and repeat the procedure until convergence is obtained. Since the dark photon lifetime is independent of the dark sector coupling constant, we derive separate limits for α_D values set to 0.1, 0.3, 0.5, 0.7, 0.9, and 1.1. The results are shown in Fig. 5 for $\alpha_D = 0.5$, and in Supplemental Material [29] for the remaining values. Bounds on the mixing strength ε down to $5 \times 10^{-5} - 10^{-3}$ are set for a large fraction of the parameter space. Constraints for different values of α_D, $m_{A'}$ and m_{Υ_D} are also shown in Fig. 6.

In summary, we report the first search for a dark sector bound state decaying into three dark photons in the range $0.001 \text{ GeV} < m_{A'} < 3.16$ GeV and $0.05 \text{ GeV} < m_{\Upsilon_D} < 9.5$ GeV. No significant signal is seen, and we derive limits on the $\gamma - A'$ kinetic mixing ε at the level of $5 \times 10^{-5} - 10^{-3}$, depending on the values of the model parameters. These measurements improve upon existing constraints over a significant fraction of dark photon masses below 1 GeV for large values of the dark sector coupling constant. Were the η_D bound state to be included in the search, the upper limits on the cross section (in the absence of a signal) could be improved by around a factor of 2, leading to an improvement on the constraints on the kinetic mixing strength by about a factor of $\sqrt{2}$.

The authors wish to thank Haipeng An and Yue Zhang for useful discussions and for providing us with MADGRAPH simulations of self-interacting dark matter processes. We also thank Gaia Lanfranchi for providing us constraints from existing experiments. We are grateful for the extraordinary contributions of our PEP-II colleagues in achieving the excellent luminosity and machine conditions that have made this work possible. The success of this project also relies critically on the expertise and dedication of the computing organizations that support *BABAR*. The collaborating institutions wish to thank SLAC for its support and the kind hospitality extended to them. This work is supported by the U.S. Department of Energy and National Science Foundation, the Natural Sciences and Engineering Research Council (Canada), the Commissariat à l'Energie Atomique and Institut National de Physique Nucléaire et de Physique des Particules (France), the Bundesministerium für Bildung und Forschung and Deutsche Forschungsgemeinschaft (Germany), the Istituto Nazionale di Fisica Nucleare (Italy), the Foundation for Fundamental Research on Matter (Netherlands), the Research Council of Norway, the Ministry of Education and Science of the Russian Federation, Ministerio de Economía y Competitividad (Spain), the Science and Technology Facilities Council (U.K.), and the Binational Science Foundation (U.S.-Israel). Individuals have received support from the Marie-Curie IEF program (European Union) and the A. P. Sloan Foundation (U.S.).

---

[*]Deceased.
[†]Present address: Wuhan University, Wuhan 430072, China.
[‡]Present address: Università di Bologna and INFN Sezione di Bologna, I-47921 Rimini, Italy.
[§]Present address: King's College, London WC2R 2LS, United Kingdom.
[‖]Present address: University of Huddersfield, Huddersfield HD1 3DH, United Kingdom.
[¶]Present address: University of South Alabama, Mobile, Alabama 36688, USA.
[**]Also at Università di Sassari, I-07100 Sassari, Italy.
[††]Also at Gran Sasso Science Institute, I-67100 LAquila, Italy.

[1] M. Pospelov, A. Ritz, and M. B. Voloshin, Phys. Lett. B **662**, 53 (2008).
[2] N. Arkani-Hamed, D. P. Finkbeiner, T. R. Slatyer, and N. Weiner, Phys. Rev. D **79**, 015014 (2009).
[3] J. Beacham *et al.*, J. Phys. G **47**, 010501 (2020).
[4] H. An, B. Echenard, M. Pospelov, and Y. Zhang, Phys. Rev. Lett. **116**, 151801 (2016).
[5] P. Fayet, Nucl. Phys. **B187**, 184 (1981).
[6] B. Holdom, Phys. Lett. **166B**, 196 (1986).
[7] F. J. Rogers, H. C. Graboske Jr., and D. J. Harwood, Phys. Rev. A **1**, 1577 (1970).
[8] E. M. Riordan *et al.* Phys. Rev. Lett. **59**, 755 (1987).
[9] J. D. Bjorken, S. Ecklund, W. R. Nelson, A. Abashian, C. Church, B. Lu, L. W. Mo, T. A. Nunamaker, and P. Rassmann, Phys. Rev. D **38**, 3375 (1988).
[10] A. Bross, M. Crisler, S. H. Pordes, J. Volk, S. Errede, and J. Wrbanek, Phys. Rev. Lett. **67**, 2942 (1991).
[11] M. Davier and H. Nguyen Ngoc, Phys. Lett. B **229**, 150 (1989).
[12] J. Blümlein and J. Brunner, Phys. Lett. B **731**, 320 (2014).
[13] D. Curtin *et al.* Phys. Rev. D **90**, 075004 (2014).
[14] J. P. Lees *et al.* (*BABAR* Collaboration), Phys. Rev. Lett. **113**, 201801 (2014).
[15] J. R. Batley *et al.* (NA48/2 Collaboration), Phys. Lett. B **746**, 178 (2015).
[16] A. Anastasi *et al.* (KLOE-2 Collaboration), Phys. Lett. B **757**, 356 (2016).
[17] D. Banerjee *et al.* (NA64 Collaboration), Phys. Rev. Lett. **120**, 231802 (2018).
[18] R. Aaij *et al.* (LHCb Collaboration), Phys. Rev. Lett. **124**, 041801 (2020).
[19] Natural units ($\hbar = c = 1$) are used throughout this Letter.
[20] J. P. Lees *et al.* (*BABAR* Collaboration), Nucl. Instrum. Methods Phys. Res., Sect. A **726**, 203 (2013).
[21] B. Aubert *et al.* (*BABAR* Collaboration), Nucl. Instrum. Methods Phys. Res., Sect. A **479**, 1 (2002).
[22] B. Aubert *et al.* (*BABAR* Collaboration), Nucl. Instrum. Methods Phys. Res., Sect. A **729**, 615 (2013).
[23] J. Alwall, R. Frederix, S. Frixione, V. Hirschi, F. Maltoni, O. Mattelaer, H. S. Shao, T. Stelzer, P. Torrielli, and M. Zaro, J. High Energy Phys. 07 (2014) 079.
[24] S. Agostinelli *et al.* (GEANT4 Collaboration), Nucl. Instrum. Methods Phys. Res., Sect. A **506**, 250 (2003).
[25] L. Breiman, Mach. Learn. **45**, 5 (2001).
[26] The helicity angle is defined as the angle between the Υ_D momentum in the center-of-mass frame and the dark photon momentum in the Υ_D rest frame.
[27] J. Berkson, J. Am. Stat. Assoc. **39**, 357 (1944).
[28] M. J. Oreglia, Ph.D. thesis, SLAC, 4158, 1981.
[29] See Supplemental Material at http://link.aps.org/supplemental/10.1103/PhysRevLett.128.021802 for additional plots about mass resolutions, classifier distribution and 90% C.L. upper limits on the signal cross section and kinetic mixing strength.
[30] W. A. Rolke, A. M. Lopez, and J. Conrad, Nucl. Instrum. Methods Phys. Res., Sect. A **551**, 493 (2005).
[31] B. Batell, M. Pospelov, and A. Ritz, Phys. Rev. D **79**, 115008 (2009).